

# XB130 Plays an Essential Role in Folliculogenesis Through Mediating Interactions Between Microfilament and Microtubule Systems in Thyrocytes

Yingchun Wang,<sup>1</sup> Yun-Yan Xiang,<sup>1,2</sup> Junichi Sugihara,<sup>1</sup> Wei-Yang Lu,<sup>2</sup> Xiao-Hui Liao,<sup>3</sup> Peter Arvan,<sup>4</sup> Samuel Refetoff,<sup>3,5,6</sup> and Mingyao Liu<sup>1,7,8</sup>

**Background:** XB130 (actin filament-associated protein 1-like 2, AFAP1L2) is a thyroid-abundant adaptor/scaffold protein. *Xb130*<sup>-/-</sup> mice exhibit transient growth retardation postnatally due to congenital hypothyroidism with diminished thyroglobulin iodination and release at both embryonic and early postnatal stages due to disorganized thyroid apical membrane structure and function. We hypothesized that XB130 is crucial for polarity and folliculogenesis by mediating proper cytoskeletal structure and function in thyrocytes.

**Methods:** Primary thyrocytes isolated from thyroid glands of *Xb130*<sup>-/-</sup> mice and their wild-type littermates at postnatal week 2 were cultured in 10% Matrigel for different time periods. Folliculogenesis was studied with immunofluorescence staining, followed by confocal microscopy. Cells were also transfected to express human XB130 fused Green Fluorescent Protein (XB130-GFP) or Green Fluorescent Protein (GFP) only before morphological analysis. Cytoskeletal structures from embryo and postnatal thyroid glands were also studied.

**Results:** In three-dimensional cultures of thyrocytes, XB130, aligned with actin filaments, participated in defining the site of apical membrane formation and coalescence to form a thyroid follicle lumen. *Xb130*<sup>-/-</sup> thyrocytes displayed delayed folliculogenesis, reduced recruitment of a microtubule (MT)-associated proteins, and disorganized acetylated tubulin under the apical membrane, resulting in delayed folliculogenesis with reduced efficiency in formation of the thyroid follicle lumen.

**Conclusions:** XB130 critically regulates thyrocyte polarization by functioning as a link between the actin filament cortex and MT network at the apical membrane of thyrocytes. Defects of adaptor scaffold proteins may affect cellular polarity and cytoskeletal structure and function and result in disorders of epithelial function, such as congenital hypothyroidism.

**Keywords:** adaptor protein, cell polarity, congenital hypothyroidism, microfilament and microtubule interaction

## Introduction

CONGENITAL PRIMARY HYPOTHYROIDISM is a condition in which the thyroid gland does not produce sufficient thyroid hormone to promote normal growth, development, and function of multiple organ systems (1). Mutations in genes that encode the cellular machinery for thyroid gland development and function have been described (2). However, mutations in the described subset of genes (or malfunction of their encoded proteins) have not

always been found in clinical cases, suggesting the presence of other yet unexplored genes and mechanisms. Defects of adaptor scaffold proteins and cytoskeletal proteins may be an important cause of epithelial dysfunction and disease, including congenital hypothyroidism. For example, the epithelial-specific clathrin adaptor protein, AP-1B, is required for Na<sup>+</sup>/I<sup>-</sup> symporter (NIS) sorting at the basolateral plasma membrane of thyrocytes, and dysfunction of AP-1B may affect iodine accumulation for thyroid hormonogenesis (3).

<sup>1</sup>Latner Thoracic Surgery Research Laboratories, Toronto General Hospital Research Institute, University Health Network, Toronto, Ontario, Canada.

<sup>2</sup>Department of Physiology and Pharmacology, University of Western Ontario, London, Ontario, Canada.

<sup>3</sup>Department of Medicine; <sup>3</sup>Department of Pediatrics; <sup>6</sup>Committee on Genetics; The University of Chicago, Chicago, Illinois, USA.

<sup>4</sup>Division of Metabolism, Endocrinology & Diabetes, University of Michigan, Ann Arbor, Michigan, USA.

<sup>7</sup>Departments of Surgery, Medicine and Physiology, and <sup>8</sup>Institute of Medical Science, Temerty Faculty of Medicine, University of Toronto, Toronto, Ontario, Canada.

Adaptor protein XB130 (actin filament-associated protein 1-like 2, AFAP1L2) is abundantly expressed in the thyroid gland (4,5). In a recent study, we reported that deficiency of XB130 results in transient postnatal growth retardation due to congenital hypothyroidism in mice. Further investigation uncovered that XB130 is highly expressed in normal thyrocytes, especially near the apical membrane. The apical membrane of thyrocytes from *Xb130*<sup>-/-</sup> mice showed reduced levels of apical-specific proteins, ezrin and thyroperoxidase, and fewer microvilli. Moreover, we reported that mutant mice exhibited reduced release of thyroglobulin (Tg) from thyrocytes to the follicle lumen and reduced iodination of Tg in the follicle lumen. We also observed more intracellular lumina and fewer central lumina in embryonic thyroid glands, suggesting delayed folliculogenesis (6). The present study was designed to further explore these defects.

Cell polarization involves organization of the cytoskeleton, which in turn facilitates the asymmetric distribution of organelles and polarized targeting of transport vesicles to the apical or basolateral membranes. Both microfilament (MF) and microtubule (MT) systems are involved in the regulation and function of polarized epithelial cells (7). However, the mechanisms of coordination of these two cytoskeletal systems are largely unknown. Adaptor proteins are involved in polarized sorting and trafficking in epithelial cells (8). With multiple protein-protein and protein-lipid interaction domains and motifs, adaptor proteins may mediate interactions between MF and MT systems. XB130 has been postulated to cross-link actin filaments (9) and interaction with other cytoskeletal proteins (10,11).

With these ideas in mind, we hypothesized that XB130, acting as an adaptor/scaffold protein, mediates MF and MT interaction and thereby plays an essential role in mediating folliculogenesis and cytoskeletal structure, which is critical to the organization of thyroid epithelial polarity and function. This hypothesis was tested first with a three-dimensional (3D), *in vitro* primary cell culture system and then results were verified with samples collected from embryonic and postnatal thyroid glands.

## Materials and Methods

### *Animal and tissue collection*

*Xb130*<sup>-/-</sup> mice were generated as previously described (12). The Animal Use and Care Committee of the University Health Network (Toronto, Canada) approved all procedures. Animals received humane care in compliance with the Guide for the Care and Use of Experimental Animals formulated by the Canadian Council on Animal Care. For tissue collection, mice were euthanized by CO<sub>2</sub> narcosis, and thyroid glands were harvested under a surgical microscope (Leica M651; Leica Microsystems, Germany).

### *Primary thyrocyte culture*

Primary thyrocytes were isolated from aseptically dissected thyroid glands of postnatal week 2 (PW2) mice and plated in Petri dishes. After a single layer of thyrocytes was formed, cells were trypsinized and mixed with 10% Matrigel (BD Biosciences, San Jose, CA). The cell-Matrigel mixture

was plated onto eight-well glass chamber slides (Thermo Fisher Scientific, Waltham, MA) and follicle structures were analyzed at various times (13).

### *Primary thyrocyte culture immunofluorescence staining*

Immunofluorescence (IF) staining of Matrigel-embedded primary thyrocyte-derived follicles was performed in an eight-well cover glass chamber (Thermo Fisher Scientific) (14). Follicles were fixed in 4% paraformaldehyde and then permeabilized with 0.025% saponin in washing solution of phosphate-buffered saline (PBS) containing 0.1 mM CaCl<sub>2</sub> and 1 mM MgCl<sub>2</sub>. Permeabilized follicles were incubated overnight in primary antibodies diluted in 0.025% saponin with 0.7% fish skin gelatin in PBS at 4°C and then incubated in secondary antibodies overnight at 4°C.

### *Human XB130-GFP transfection*

Human XB130-GFP or GFP-only vector (11) was transfected into *Xb130*<sup>-/-</sup> primary thyrocytes using Lipofectamine 3000 and cultured in a six-well tissue culture plate for three days. One day after transfection, thyrocytes were trypsinized and cultured in Matrigel for another 48–72 hours. Follicles were fixed for morphological analysis.

### *Embryo harvest*

Breeding pairs of *Xb130*<sup>+/-</sup> mice were set up for timed pregnancy. Embryos were collected at different gestation stages, fixed in 10% formalin, and embedded in paraffin. For immunostaining, embryo samples from two to four litters were collected for each developmental stage.

### *Tissue IF studies and quantification*

For IF staining, paraffin or frozen sections were incubated with primary antibodies and then secondary antibodies. Slides were counterstained with 4',6-diamidino-2'-phenylindole (Invitrogen) and mounted with SlowFade. IF staining of embryonic tissues was visualized under a Nikon AIR+ confocal microscope, and acquisition and analysis were performed using NIS-Elements C software (Nikon Instruments, Inc., New York, NY). Some image acquisition and analyses were performed using Olympus FluoView 1000B.

### *Immunoblotting*

Using TissueLyser II (Qiagen, Valencia, CA), thyroid tissues were homogenized in RIPA buffer supplemented with protease and phosphatase inhibitors. Protein concentration of tissue lysates was measured using the Pierce BCA Protein Assay Kit (Thermo Fisher Scientific). Tissue lysates with equal volume of total proteins were loaded and separated by SDS-PAGE (sodium dodecyl sulfate-polyacrylamide gel electrophoresis) and then electrotransferred to nitrocellulose membranes. Membranes were blocked for one hour at room temperature in 5% skim milk. Primary and secondary antibodies were used for immunoblotting. Proteins were revealed using SuperSignal West Dura Chemiluminescent Substrate (Thermo Fisher Scientific).

### Statistical analysis

Comparison of the percentage of incidence was performed using unpaired T-Test. Data are presented as mean  $\pm$  standard error of the mean;  $p < 0.05$  is considered statistically significant.

## Results

### Delayed folliculogenesis in 3D culture of thyrocytes from *Xb130*<sup>-/-</sup> mice

To determine whether the defects of folliculogenesis observed in thyroid glands from *Xb130*<sup>-/-</sup> mice (6) are cell autonomous, we used a 3D system to culture primary thyrocytes isolated from PW2 mice *in vitro*. Folliculogenesis can be divided into 10 steps in 3D cultures (15,16). We used phalloidin to highlight actin filaments,  $\beta$ -catenin for the basolateral membrane, and ezrin for the apical membrane. In thyrocytes from *Xb130*<sup>+/+</sup> mice, intracellular lumina appeared as early as during the first cell division, followed by polarized two-cell follicle, polarized growing follicle, and functional polarized follicle stages (Fig. 1A). At the two-cell stage, XB130 first appeared together with  $\beta$ -catenin/actin filaments around the cytoplasmic membrane (Fig. 1B-3) and then at the interface between two daughter cells (Fig. 1B-4). Later, actin filaments were focally enriched at the apical membrane initiation site (AMIS) (17), whereas  $\beta$ -catenin and XB130 were found at both the AMIS and in peripheral cytoplasmic membranes (Fig. 1B-5). Next, a preapical patch (PAP) emerged between the two cells, which featured enhanced actin filaments and selective preferential accumulation of XB130, but not selective preferential accumulation of  $\beta$ -catenin (Fig. 1B-6). Indeed, at later stages,  $\beta$ -catenin gradually disappeared from the apical site and moved toward the basolateral membranes of the follicle structure, whereas XB130 remained enriched, together with actin filaments, along the apical rings of both intracellular and central lumina (Fig. 1B-7, B-8, and B-10). When intracellular lumina fused into a central lumen, ezrin disappeared at the fusion site and only located on the apical membrane (Fig. 1C), while XB130 was seen together with actin filaments at both the fusion site and apical membrane (Fig. 1B-8 and data not shown), indicating that XB130 is preferentially associated with actin filaments rather than with ezrin (an apical-specific membrane marker).

When *Xb130*<sup>-/-</sup> thyrocytes were transfected with a construct expressing only GFP, a diffuse cytoplasmic distribution was observed (Fig. 2A). In cells transfected with human XB130 fused with GFP (hXB130-GFP), fluorescence was noted at both intracellular and central lumina, colocalized with ezrin (Fig. 2B) and phalloidin (Fig. 2C). These results indicate that XB130 is closely associated with the membrane actin network during folliculogenesis and tagged human XB130 appears to have a similar or identical localization to that of endogenous murine XB130.

After 10 days of culture, even though both intracellular lumina and mature central lumina were observed in thyrocyte aggregates of both genotypes (Fig. 1D), the incidence of central lumina was significantly lower in cultures derived from *Xb130*<sup>-/-</sup> thyrocytes (Fig. 1E). Iodinated Tg (I-Tg) was detected in both intracellular and central lumina in cells derived from *Xb130*<sup>+/+</sup> mice, and those from *Xb130*<sup>-/-</sup>

mice exhibited a significantly lower level of I-Tg staining (Fig. 1F). Thus, XB130 is involved in the folliculogenesis and function of the follicle lumen—including iodination of Tg.

### Disorganized MT network in 3D cell culture of thyrocytes from *Xb130*<sup>-/-</sup> mice

We then investigated in greater detail the relationship between XB130 and other apical proteins using confocal microscopy. Briefly, in the intracellular or central lumina, XB130 staining was immediately outward adjacent with partial overlap of ezrin rings (Fig. 3A, top panel, and Supplementary Fig. S1). XB130 was colocalized with the actin filament ring (Fig. 3A, middle panel) and was on the luminal side adjacent to acetylated tubulin (Fig. 3A, lower panel, and Supplementary Fig. S2). This molecular pattern of the ezrin-actin-XB130-tubulin arrangement suggests an important role of XB130 in helping to connect the apical actin cortex to the microtubular network.

In polarized epithelial cells, calmodulin-regulated spectrin-associated proteins (CAMSAPs) play a key role in tethering MTs to the apical cortex (18,19). We reasoned that XB130 might be involved in the organization of MTs under the thyrocyte apical membrane through recruitment of CAMSAPs. CAMSAP2 regulates the organization of cellular organelles, including the Golgi network and early endosomes (20). Dense IF of CAMSAP2 was found primarily on the apical membrane of thyrocytes from *Xb130*<sup>+/+</sup> mice and colocalized with the circumferential acetylated tubulin around the lumen. In contrast, in thyrocytes from *Xb130*<sup>-/-</sup> mice, localization of acetylated tubulin was disrupted, along with diminished apical selectivity of CAMSAP2 (Fig. 3B, C).

CAMSAP3 is required for orienting the apical-to-basal polarity of MTs in epithelial cells, acting by tethering non-centrosomal MTs to the apical cortex, leading to their longitudinal orientation (18,21). In aggregates of thyrocytes from *Xb130*<sup>+/+</sup> mice, CAMSAP3 was enriched at the apical membrane, being largely colocalized with the actin ring (Fig. 3D) and acetylated tubulin around the lumen (Fig. 3E). Notably, CAMSAP3 immunostaining was significantly reduced at the apical pole of cells from *Xb130*<sup>-/-</sup> mice (Fig. 3D, E). Loss of polarized MT arrays has been observed in CAMSAP3-deficient intestinal epithelial cells (21); thus, reduced expression of CAMSAP3 on the apical membrane in *Xb130*<sup>-/-</sup> thyrocytes is likely to affect their MT network as well (Fig. 3F).

MTs in epithelial cells play important roles in establishing cell polarity by forming a dense network under the apical pole, with their minus ends facing the apical surface and plus ends facing the basolateral surface. In this way, MTs provide trails for apical cargo trafficking and maintenance of cell morphology (22). Furthermore, the acetylation of tubulin directly tunes the compliance and resilience of MTs (23). During thyroid folliculogenesis, acetylated tubulin propagated radially around the intracellular lumina, both perpendicularly and circumferentially. As these luminal structures coalesced in 3D culture, circumferential acetylated tubulin nets fused together and gradually formed a circular or oval-shaped central lumen (Fig. 4A). In 3D cultures of thyrocytes from *Xb130*<sup>-/-</sup> mice, the number of lumina with dense circumferential acetylated tubulin was significantly lower (Fig. 4B) and the number of irregular central lumina of thyroid follicles was significantly higher than those in cells from *Xb130*<sup>+/+</sup> mice (41.7% vs. 17.6%,  $p = 0.03$ ).

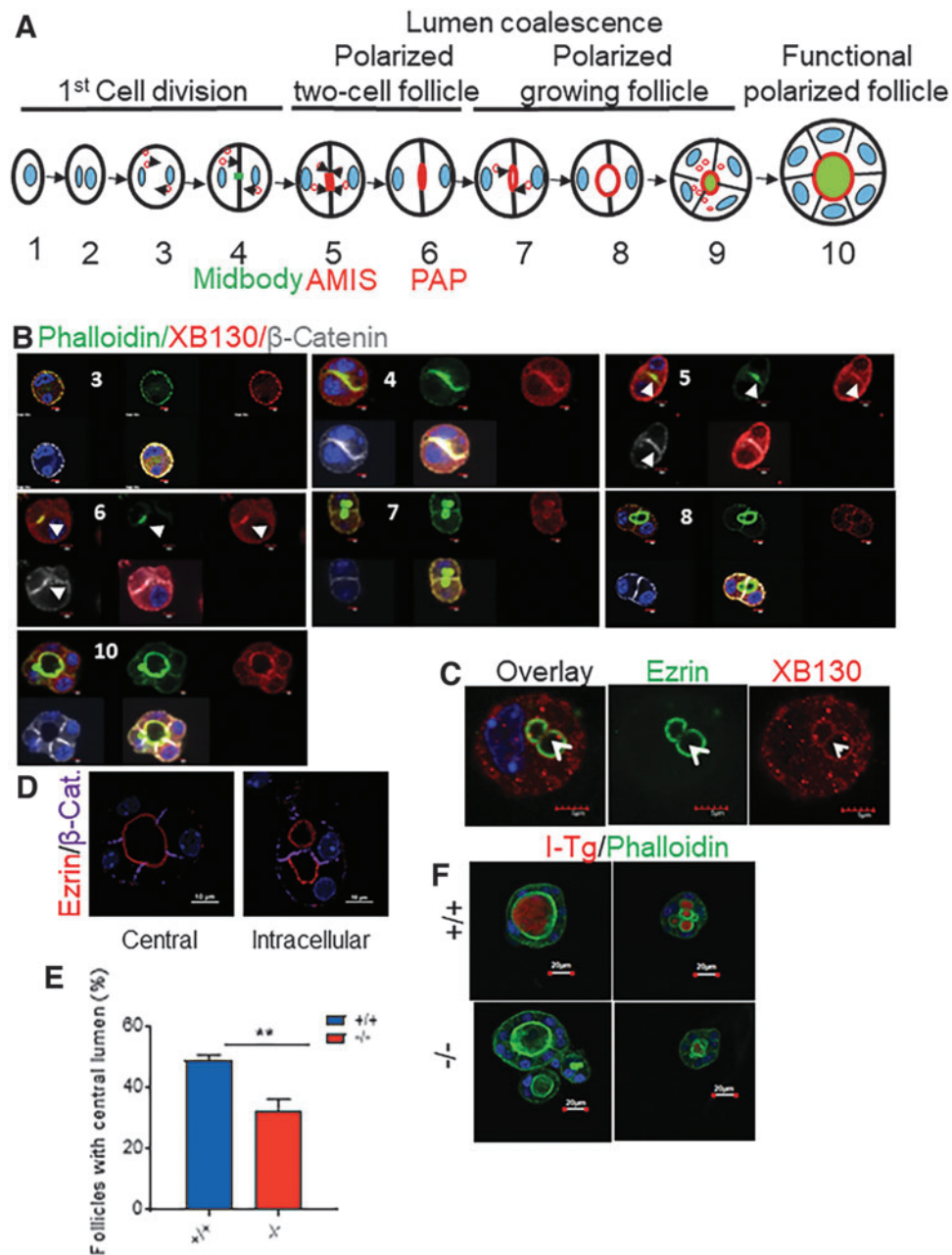


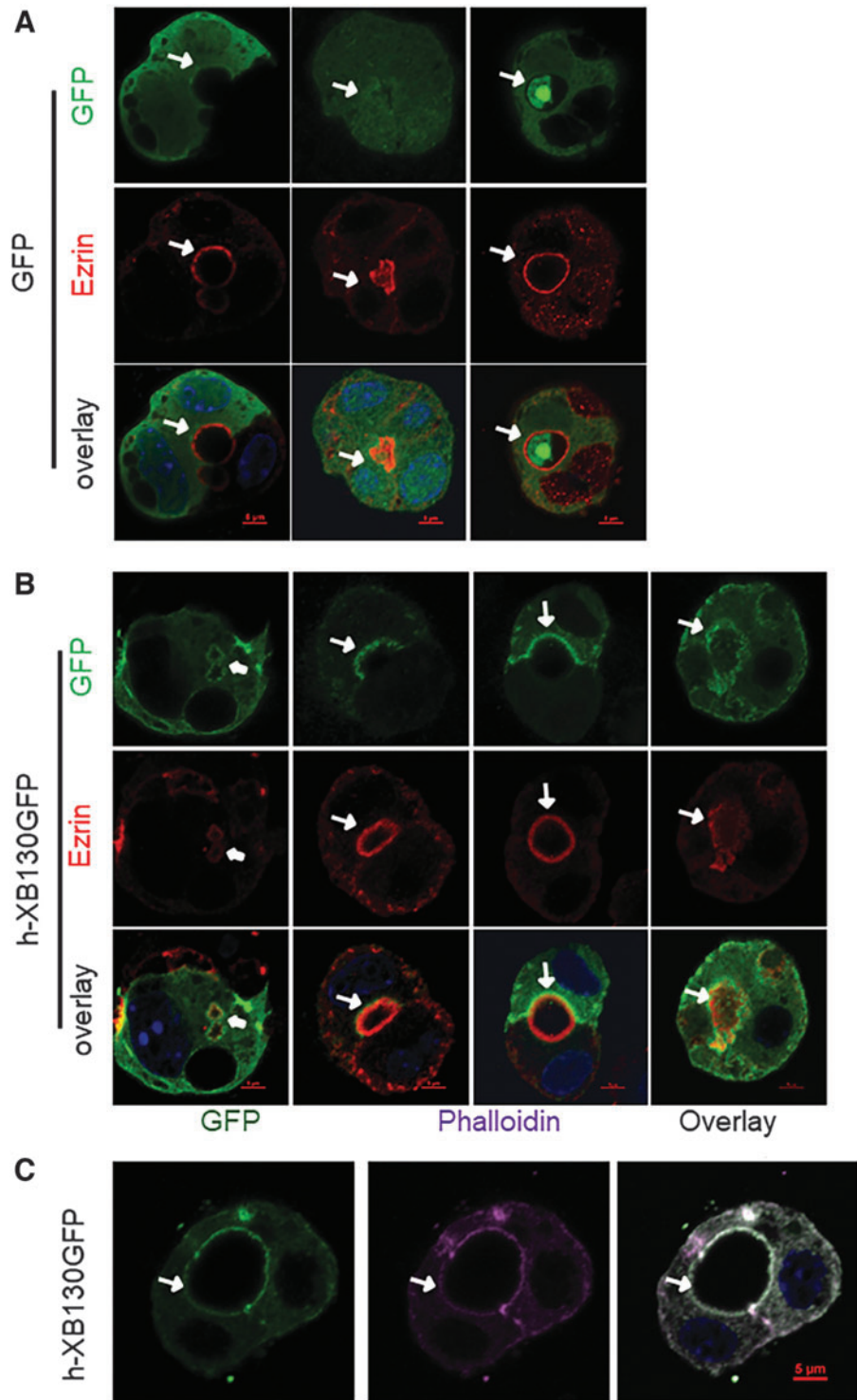
**FIG. 1.** Delayed central lumen formation and lack of I-Tg in lumen-like structure in 3D culture of thyrocytes from *Xb130*<sup>-/-</sup> mice. (A) Schematic illustration of major steps of lumen coalescence. (B–D) Primary thyrocytes were harvested from thyroid glands of PW2 *Xb130*<sup>+/+</sup> mice and cultured in Matrigel for a varied period of time before IF staining. (B) IF staining to show actin filaments with phalloidin and membrane structure with  $\beta$ -catenin to determine XB130 at different stages of lumen coalescence. Number shows the step in lumen coalescence. Arrows indicate AMIS or PAP. (C) Double staining of ezrin/XB130 at the lumen coalescence site. Arrowhead shows the separation of ezrin and XB130 at the fusion site. (D) Intracellular lumen (right) and a central lumen (left) were revealed by ezrin/ $\beta$ -catenin staining. (E) The ratio of follicles with a single central lumen versus follicles containing intracellular lumens from thyrocytes harvested from PW2 mice and cultured in Matrigel for 10 days. Results are from four independent experiments. In total, >400 follicles were counted in each group. (F) Representative image of IF staining of I-Tg. Primary thyrocytes were cultured in Matrigel for 10 days, and NaI was added to the culture medium for another 5 days. Data are presented as mean  $\pm$  SEM. \*\* $p < 0.01$ . 3D, three-dimensional; AMIS, apical membrane initiation site; I-Tg, iodinated thyroglobulin; IF, immunofluorescence; PAP, preapical patch; PW2, postnatal week 2; SEM, standard error of the mean. Color images are available online.

#### Disorganized MTs in thyroid glands from *Xb130*<sup>-/-</sup> mice

In thyroid glands of PW2 *Xb130*<sup>+/+</sup> mice, most follicles showed enrichment of the acetylated tubulin mesh under the

apical membrane, forming a continuous ring along the luminal rim, with weak staining of short bundles along the lateral membrane near the apical site (Fig. 5A). In contrast, most follicles in thyroid glands from *Xb130*<sup>-/-</sup> mice lacked a continuous apical ring of acetylated tubulin, instead

**FIG. 2.** hXB130-GFP is recruited to intracellular and central lumens when expressed in *Xb130*<sup>-/-</sup> thyrocytes in 3D culture. Primary thyrocytes harvested from *Xb130*<sup>-/-</sup> mice at PW2 were cultured for three days in a six-well plate and then transfected with vector containing GFP or human XB130 tagged with GFP. At 24 hours post-transfection, cells were harvested and cultured in Matrigel for 2–3 days. (A, B) Thyrocytes were stained with ezrin/GFP. (C) Thyrocytes were stained with phalloidin/GFP. Arrows: cell interphase and central lumen; arrowheads: intracellular lumen. Color images are available online.



exhibiting enhanced staining of elongated bundles in the cytoplasm, especially longitudinally parallel to or along the lateral membrane (Fig. 5A). Immunoblotting assays confirmed higher expression of both  $\alpha$ -tubulin and acetylated tubulin in the thyroid glands of PW2 and PW14 *Xb130*<sup>-/-</sup> mice (Fig. 5B).

The increased expression and altered distribution pattern of acetylated tubulin in thyroid glands from *Xb130*<sup>-/-</sup> mice

were also observed during embryonic stages. In thyroid glands of E15.5 *Xb130*<sup>+/+</sup> mice, the IF staining of acetylated tubulin in follicles predominantly localized at the apical tips between adjacent thyrocytes, appearing as a dotted ring along the follicular lumen (Fig. 5C). In thyroid glands from *Xb130*<sup>-/-</sup> mice, however, acetylated tubulin was bundled on the lateral membrane of thyrocytes, projecting longitudinally from the apical rings to the basal end (Fig. 5C). In thyroid

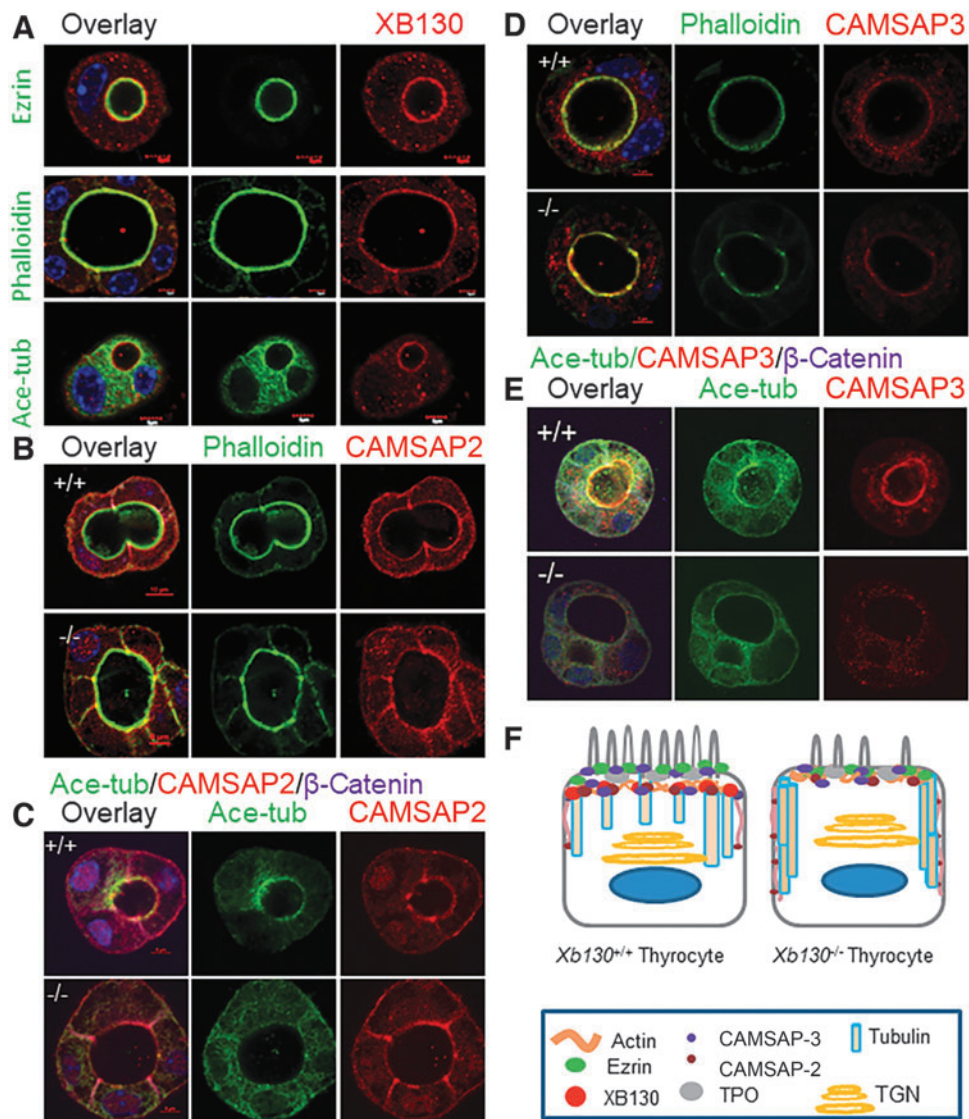


**FIG. 3.** Distribution of microtubule-binding proteins on the apical membrane of thyrocytes in 3D culture. Primary thyrocytes from PW2 mice were cultured in Matrigel for 10 days. Representative IF images are shown. (A) Double staining of XB130 with ezrin, phalloidin, or acetylated tubulin. (B) CAMSAP2/phalloidin double staining. (C) CAMSAP2/acetylated tubulin/ $\beta$ -catenin triple staining. (D) CAMSAP3/phalloidin double staining. CAMSAP3 on the apical membrane was reduced in the *Xb130*<sup>-/-</sup> group of mice. (E) CAMSAP3/acetylated tubulin/ $\beta$ -catenin triple staining. CAMSAP3 was adjunctive to the circumferential acetylated tubulin around the lumen and staining on the apical membrane was reduced in the *Xb130*<sup>-/-</sup> group of mice. (F) A schematic diagram to show apical proteins and apical cytoskeletal structure in thyrocytes. Color images are available online.

glands of E18.5 *Xb130*<sup>+/+</sup> mice, acetylated tubulin again appeared predominantly as a continuous ring under the apical membrane, whereas in thyroid glands from *Xb130*<sup>-/-</sup> mice, staining of acetylated tubulin was significantly stronger and distributed along the lateral membrane (Fig. 5D). The increased abundance of disorganized acetylated tubulin may alter its function (Fig. 5E, see the Discussion section).

## Discussion

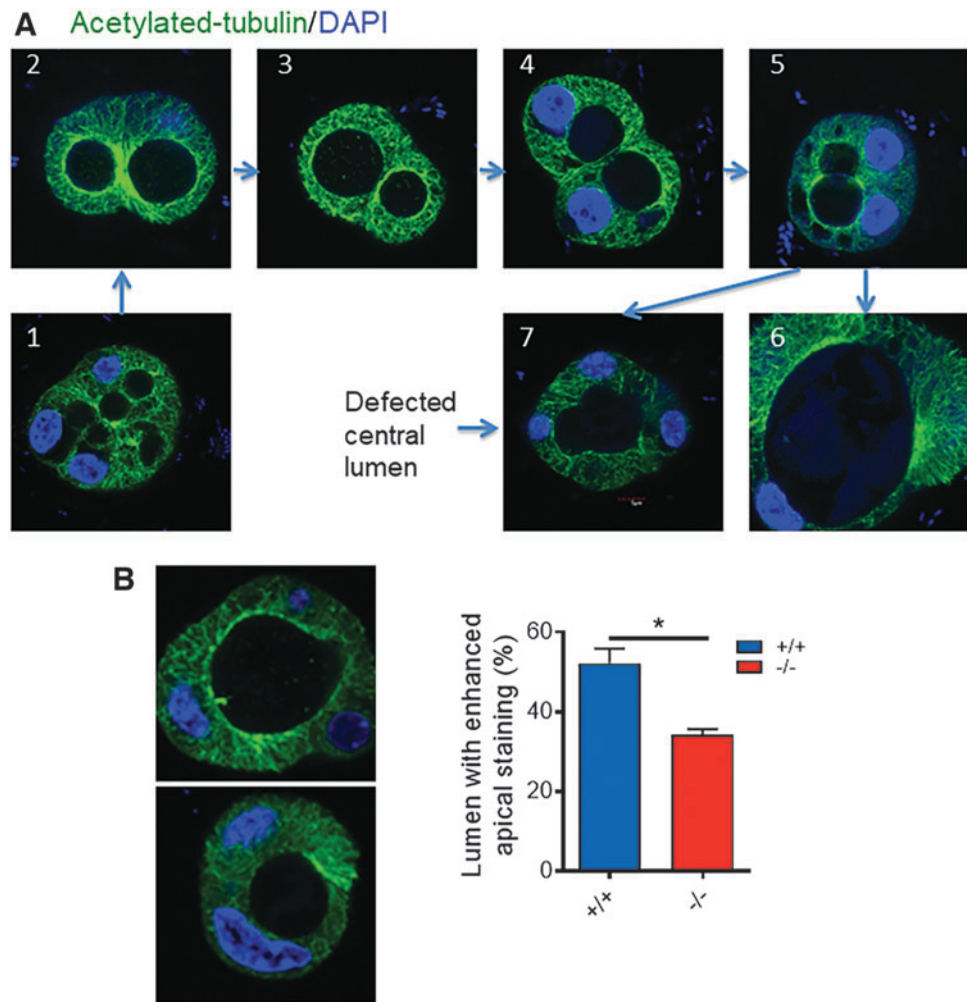
The present study demonstrated crucial roles of XB130 in folliculogenesis of thyrocytes and in regulating the structure and function of the thyroid apical membrane, through coordinating interactions between MF and MT systems. These observations support the significance of adaptor/scaffold proteins and cytoskeletal systems in maintaining the physiological function of epithelia, such as seen in the thyroid glands from the current study. Disorder or dysfunction of these proteins may contribute to the pathogenesis of epithelial diseases such as congenital hypothyroidism in *Xb130*<sup>-/-</sup> mice (6).

## *XB130 is involved in folliculogenesis of thyrocytes*

Proper intracellular trafficking and fusion of intracellular lumina to the apical initiation site are critical for the formation of a central thyroid follicular luminal cavity. In the 3D cell culture, XB130 was closely associated with actin filaments during folliculogenesis, starting at the interface between two adjacent cells, at the AMIS and PAP, and from the intracellular lumina to the central lumen. It is known that XB130 has high affinity to the cortical filament network (10,11). Interestingly, when two adjacent luminal structures merged together, ezrin, a specific marker for the apical membrane, disappeared from the fusion site, whereas XB130 was observed at both the fusion site and apical membrane structure together with actin filaments. This suggests that XB130 is specifically associated with the actin filament network in thyrocytes.

In the *Xb130*<sup>-/-</sup> cell culture, the steps of folliculogenesis are also observed (data not shown), suggesting that XB130 is not necessary for this process. However, lack of XB130 delayed thyroid folliculogenesis and resulted in misshapen

**FIG. 4.** Disorganized microtubules of *Xb130*<sup>-/-</sup> thyrocytes in 3D culture. (A) Acetylated tubulin IF staining (green) in 3D culture of primary thyrocytes. Examples of coalescence of the intracellular lumen to form a central lumen. (1) Cells with multiple intracellular lumina; (2) two adjacent lumina with strong acetylated tubulin staining; (3) staining is less in one lumen than another; (4) thinning of acetylated tubulin between two adjacent lumina; (5) disappearance of separation between two lumina; (6) formation of one oval central lumen; and (7) defective central lumen (significantly high percentage in *Xb130*<sup>-/-</sup> thyrocytes,  $p = 0.03$ ). (B) Acetylated tubulin staining. Left: lumen with or without enriched apical acetylated tubulin staining. Right: the ratio of lumens with enriched apical acetylated tubulin staining was significantly lower in the *Xb130*<sup>-/-</sup> group. Data are mean  $\pm$  SEM, \* $p < 0.05$ . Total numbers of lumens counted:  $n = 90$  in the *Xb130*<sup>+/+</sup> group and  $n = 104$  in the *Xb130*<sup>-/-</sup> group, pooled from three experiments. Color images are available online.



central lumens at late embryonic stages. Fewer microvilli on the apical surface of follicles and enriched intracellular lumina in thyrocytes were also shown by transmission electron microscopy from *Xb130*<sup>-/-</sup> mice at PW2, suggesting that folliculogenesis is affected in postnatal mice as well (6). XB130, together with MFs, may be involved in the formation and fusion of these structures at the apical membrane in follicles, helping to recruit apical membrane proteins such as ezrin and thyroperoxidase, as well as apical membrane function such as Tg iodination and release (6).

#### *XB130 regulates thyrocyte polarity possibly by mediating interactions between MF and MT systems*

Intracellular vesicular trafficking is mediated by specific vesicle transport complexes, which involve multiple protein components and are regulated by a functional cytoskeletal network of MFs and MTs (24). MT integrity is essential for apical polarization and epithelial morphogenesis in the thyroid gland (25). The relationship of ezrin, the actin filament network, XB130, and tubulin at the apical membrane of thyrocytes further supports its role in mediating interactions between MF and MT systems.

In intestinal epithelial cells, MT minus ends were stabilized by CAMSAP3 at the apical membrane (18). In thyrocytes from *Xb130*<sup>-/-</sup> mice, staining of CAMSAP3 was significantly reduced on the apical membrane surrounding the central lumen. Moreover, the distribution pattern of CAMSAP2 in thyrocytes from *Xb130*<sup>-/-</sup> mice is also different from that of *Xb130*<sup>+/+</sup> thyrocytes, implying that XB130 directly or indirectly affects the recruitment of CAMSAP3 and other MT-binding proteins to the apical membrane structure and subsequently affects the anchorage (and stability) of MTs to the actin filament network. Both 3D cell culture and *in vivo* studies showed that the lack of XB130 altered apical tubulin acetylation and organization in thyrocytes. This may affect the transport of vesicles between the cytoplasm and apical plasma membrane, which may account for much of the dysfunction observed in the current and previous studies on thyroid glands from *Xb130*<sup>-/-</sup> mice (6).

#### *Limitations and future studies*

In the current study, we focused on apical membrane structure and function. Ideally, we would have liked to examine NIS as a control to determine basal membrane

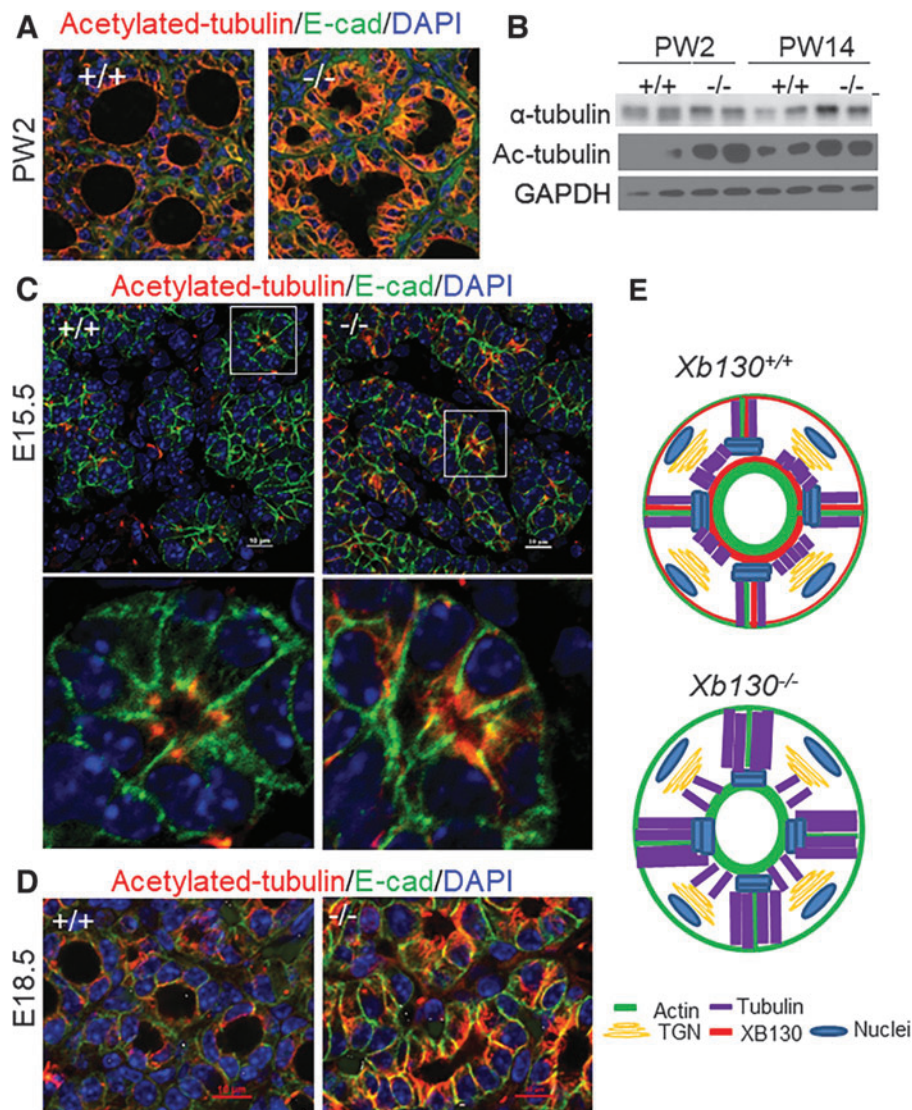


**FIG. 5.** Disorganized microtubules in postnatal and embryonic thyroid glands in *Xb130*<sup>-/-</sup> mice. **(A, C, D)** IF staining of acetylated tubulin in thyroid glands at different developmental stages. **(A)** At PW2, enhanced staining especially in the cytoplasm along the lateral membrane is seen in thyrocytes from *Xb130*<sup>-/-</sup> mice, with irregular follicle lumen structures ( $n=6$  mice in each group). **(B)** Protein expression of  $\alpha$ -tubulin and acetylated tubulin in the thyroid gland of postnatal mice. Each lane represents a pool of three to four thyroid glands. **(C)** E15.5. Upper: low magnification. Lower: high magnification of the image in the white box. Increased staining is seen in thyrocytes from *Xb130*<sup>-/-</sup> mice ( $n=8-11$  mice in each group). **(D)** E18.5. Enhanced staining of elongated microtubule bundles in the cytoplasm, longitudinally parallel to or along the lateral membrane, is seen in thyrocytes from *Xb130*<sup>-/-</sup> mice ( $n=4-6$  mice in each group). **(E)** Proposed models of acetylated tubulin distribution in thyroid follicles from *Xb130*<sup>+/+</sup> or from *Xb130*<sup>-/-</sup> mice. Color images are available online.

polarity and this will be explored in future studies. However, we note that PECAM (an endothelial cell marker) showed proper staining near the basal membrane of thyrocytes in thyroid glands from both *Xb130*<sup>+/+</sup> and *Xb130*<sup>-/-</sup> mice (6). Moreover, we did not observe any inverted polarity in follicles. The morphology of follicles between thyroid glands from *Xb130*<sup>+/+</sup> and *Xb130*<sup>-/-</sup> mice is generally similar, with a monolayered status maintained in surviving follicles (6).

In thyroid cancer studies, XB130 has been found as a substrate for RET/PTC (rearrangements of the rearranged during transfection [RET] proto-oncogene in papillary histotype) oncogenic kinase (5) and multiple protein tyrosine kinases (26). Association of XB130 with the p85 $\alpha$  subunit of phosphatidylinositol-3 kinase has been reported and may activate Akt and downstream signals to mediate tumor cell growth (26,27). XB130 also regulates expression of tumor-suppressive microRNAs in thyroid cancer cells (28). XB130 contains multiple protein-protein and protein-lipid interaction domains/motifs and protein phosphorylation sites (29). Therefore, the role of XB130 protein phosphorylation

and its role in downstream signaling are fertile areas for future study.

Taken together, data from the present study highly suggest that XB130 actively interacts with actin filaments during thyroid folliculogenesis. Lack of XB130 not only slows down this process but also reduces the iodination of Tg released into both intracellular and central lumina. XB130 also mediates interactions between MF and MT networks in thyrocytes. Disorganized cell polarity results in complex dysfunction during embryonic and postnatal development, eventually leading to congenital hypothyroidism with transient postnatal growth retardation. Disorders of the adaptor/scaffold protein and cytoskeletal structure, cell polarity, and basal/apical membrane structure and function should be further explored as potential pathogenic mechanisms of congenital hypothyroidism.

#### Acknowledgment

The authors thank Dr. Masatoshi Takeich for providing antibodies and advice.



### Authors' Contributions

M.L. and Y.W. designed the project and wrote the manuscript. Y.W. participated in most of the experiments. Y.-Y.X. participated in immunofluorescence studies. J.S. and X.-H.L. helped to prepare and edit the manuscript. S.R., P.A., and W.-Y.L. provided conceptual advice, planned some of the experiments, and edited the manuscript. All coauthors have approved the manuscript for submission.

### Author Disclosure Statement

No competing financial interests exist.

### Funding Information

This research was supported by grants from the Canadian Institutes of Health Research (MOP-31227, MOP-42546, and MOP-119514 to Mingyao Liu) and from the National Institutes of Health, DK15070 (to Samuel Refetoff) and DK40344 (to Peter Arvan). Mingyao Liu is James and Mary Davie Chair in Lung Injury, Repair and Regeneration.

### Supplementary Material

Supplementary Figure S1

Supplementary Figure S2

### References

- Wassner AJ 2018 Congenital hypothyroidism. *Clin Perinatol* **45**:1–18.
- Grasberger H, Refetoff S 2011 Genetic causes of congenital hypothyroidism due to dysmorphogenesis. *Curr Opin Pediatr* **23**:421–428.
- Martín M, Modenutti CP, Peyret V, Geysels RC, Darrouzet E, Pourcher T, Masini-Repiso AM, Martí MA, Carrasco N, Nicola JP, 2019 A carboxy-terminal monoleucine-based motif participates in the basolateral targeting of the Na<sup>+</sup>/I<sup>-</sup>symporter. *Endocrinology* **160**:156–168.
- Xu J, Bai XH, Lodyga M, Han B, Xiao H, Keshavjee S, Hu J, Zhang H, Yang BB, Liu M 2007 XB130, a novel adaptor protein for signal transduction. *J Biol Chem* **282**:16401–16412.
- Lodyga M, De Falco V, Bai X, Kapus A, Melillo RM, Santoro M, Liu M 2009 XB130, a tissue-specific adaptor protein that couples the RET/PTC oncogenic kinase to PI 3-kinase pathway. *Oncogene* **28**:937–949.
- Wang Y, Shimizu H, Xiang Y, Sugihara J, Lu W, Liao X, Cho H, Toba H, Bai XH, Asa S, Arvan P, Refetoff S, Liu M 2021 XB130 deficiency causes congenital hypothyroidism in mice due to disorganized apical membrane structure and function of thyrocytes. *Thyroid* **31**:1650–1661.
- Apodaca G 2001 Endocytic traffic in polarized epithelial cells: role of the actin and microtubule cytoskeleton. *Traffic* **2**:149–159.
- Bonifacino JS 2014 Adaptor proteins involved in polarized sorting. *J Cell Biol* **204**:7–17.
- Yamanaka D, Akama K, Chida K, Minami S, Ito K, Hakuno F, Takahash S 2016 Phosphatidylinositol 3-kinase-associated protein (PI3KAP)/XB130 crosslinks actin filaments through its actin binding and multimerization properties in vitro and enhances endocytosis in HEK293 cells. *Front Endocrinol (Lausanne)* **7**:89.
- Wu Q, Nadesalingam J, Moodley S, Bai XH, Liu M 2015 XB130 translocation to microfilamentous structures mediates NNK-induced migration of human bronchial epithelial cells. *Oncotarget* **6**:18050–18065.
- Moodley S, Derouet M, Bai XH, Xu F, Kapus A, Yang BB, Liu M 2016 Stimulus-dependent dissociation between XB130 and Tks5 scaffold proteins promotes airway epithelial cell migration. *Oncotarget* **7**:76437–76452.
- Zhao J, Wang Y, Wakeham A, Hao Z, Toba H, Bai XH, Keshavjee S, Mak T, Liu M 2014 XB130 deficiency affects tracheal epithelial differentiation during airway repair. *PLoS One* **9**:e108952.
- Jeker LT, Hejazi M, Burek CL, Rose NR, Caturegli P 1999 Mouse thyroid primary culture. *Biochem Biophys Res Commun* **257**:511–515.
- Yu W, Datta A, Leroy P, O'Brien LE, Mak G, Jou T, Matlin KS, Mostov KE, Zegers MMP 2005 Beta1-integrin orients epithelial polarity via Rac1 and laminin. *Mol Biol Cell* **16**:433–445.
- Bryant DM, Datta A, Rodríguez-Fraticelli AE, Peränen J, Martín-Belmonte F, Mostov KE 2010 A molecular network for de novo generation of the apical surface and lumen. *Nat Cell Biol* **12**:1035–1045.
- Datta A, Bryant DM, Mostov KE 2011 Molecular regulation of lumen morphogenesis. *Curr Biol* **21**:R126–R136.
- Mangan AJ, Sietsema DV, Li D, Moore JK, Citi S, Prekeris R 2016 Cingulin and actin mediate midbody-dependent apical lumen formation during polarization of epithelial cells. *Nat Commun* **7**:12426.
- Noordstra I, Liu Q, Nijenhuis W, Hua S, Jiang K, Baars M, Remmelzwaal S, Martin M, Kapitein L, Akhmanova A 2016 Control of apico-basal epithelial polarity by the microtubule minus-end-binding protein CAMSAP3 and spectraplakins ACF7. *J Cell Sci* **129**:4278–4288.
- Tanaka N, Meng W, Nagae S, Takeichi M 2012 Nezha/CAMSAP3 and CAMSAP2 cooperate in epithelial-specific organization of noncentrosomal microtubules. *Proc Natl Acad Sci U S A* **109**:20029–20034.
- Wu J, de Heus C, Liu Q, Bouchet BP, Noordstra I, Jiang K, Hua S, Martin M, Yang C, Grigoriev I, Katrukha EA, Altelaar AFM, Hoogenraad CC, Qi RZ, Klumperman J, Akhmanova A 2016 Molecular pathway of microtubule organization at the Golgi apparatus. *Dev Cell* **39**:44–60.
- Toya M, Kobayashi S, Kawasaki M, Shioi G, Kaneko M, Ishiuchi T, Misaki T, Meng W, Takeichi M 2016 CAMSAP3 orients the apical-to-basal polarity of microtubule arrays in epithelial cells. *Proc Natl Acad Sci U S A* **113**:332–337.
- Musch A 2004 Microtubule organization and function in epithelial cells. *Traffic* **5**:1–9.
- Palazzo A, Ackerman B, Gundersen GG 2003 Cell biology: tubulin acetylation and cell motility. *Nature* **421**:230.
- Hehnlly H, Stamnes M 2007 Regulating cytoskeleton-based vesicle motility. *FEBS Lett* **581**:2112–2118.

25. Yap AS, Manley SW 2001 Microtubule integrity is essential for apical polarization and epithelial morphogenesis in the thyroid. *Cell Motil Cytoskeleton* **48**:201–212.
26. Shiozaki A, Lodyga M, Bai XH, Nadesalingam J, Oyaizu T, Winer D, Asa S, Keshavjee S, Liu M 2011 XB130, a novel adaptor protein, promotes thyroid tumor growth. *Am J Pathol* **178**:391–401.
27. Shiozaki A, Shen-Tu G, Bai XH, Iitaka D, De Falco V, Santoro M, Keshavjee S, Liu M 2012 XB130 mediates cancer cell proliferation and survival through multiple signal events downstream of Akt. *PLoS One* **7**:e43646.
28. Takeshita H, Shiozaki A, Bai XH, Iitaka D, Kim H, Yang BB, Keshavjee S, Liu M 2013 XB130, a new adaptor protein, regulates expression of tumor suppressive micro-RNAs in cancer cells. *PLoS One* **8**:e59057.
29. Bai XH, Cho H, Moodley S, Liu M 2014 XB130—a novel adaptor protein: gene, function, and roles in tumorigenesis. *Scientifica (Cairo)* **2014**:903014.

Address correspondence to:  
*Mingyao Liu, MD*  
*Department of Surgery Medicine*  
*Institute of Medical Science*  
*Temerty Faculty of Medicine*  
*University of Toronto*  
*101 College Street, Room: PMCRT2-814*  
*Toronto, ON M5G 1L7*  
*Canada*

*E-mail: mingyao.liu@utoronto.ca*